Complex relationship between TCTP, microtubules and actin microfilaments regulates cell shape in normal and cancer cells

Franck Bazile [1] , Aude Pascal [1] , Isabelle Arnal [2] , Christophe Le Clainche [3] , Franck Chesnel [1] , Jacek Z. Kubiak [1 *]

[1] *IGDR, Institut de Génétique et Développement de Rennes CNRS : UMR6061 , Université de Rennes I , IFR140 , Faculté de Médecine - CS 34317 2 Av du Professeur Léon Bernard 35043 RENNES CEDEX,FR*

[2] *ICM, Interactions cellulaires et moléculaires CNRS : UMR6026 , Université de Rennes I , IFR140 , bat. 13 et 14 Campus de Beaulieu 35042 RENNES CEDEX,FR*

[3] *Laboratoire d'Enzymologie et Biochimie Structurales CNRS : FRE 2930 , Gif sur Yvette,FR*

* Correspondence should be adressed to: Jacek Kubiak <Jacek.Kubiak@univ-rennes1.fr >

Abstract

Translationally Controlled Tumor-associated Protein (TCTP) is a ubiquitous and highly conserved protein implicated in cancers. Here we demonstrate that interactions of TCTP with microtubules (MTs) are functionally important but indirect, and we reveal novel interaction of TCTP with the actin cytoskeleton. Firstly, immunofluorescence in Xenopus XL2 cells revealed cytoplasmic fibers stained with TCTP but not with tubulin antibodies, as well as MT-free of TCTP. Furthermore, TCTP localized to a subset of actin-rich fibers in migrating cells. Secondly Xl TCTP did not affect in vitro assembly/disassembly of MTs, and lacked MT binding affinity both in pull-down assays and in cell-free extracts. Although TCTP also failed to bind to purified F-actin, it associated with microfilaments in cell-free extracts. Thirdly, TCTP concentrated in mitotic spindle did not colocalize with MTs, and was easily dissociated from these structures except at the poles. Finally, RNAi knockdown of TCTP in XL2 and HeLa cells provoked drastic, MT-dependent, shape change. These data show that although TCTP interacts with MTs it does not behave as classic MT Associated Protein (MAP). Our evidence for an association of TCTP with F-actin structures, and for an involvement in cell shape regulation, implicates this protein in integrating cytoskeletal interations both in interphase and mitosis providing a new avenue to fully understand the role of TCTP.

MESH Keywords Animals ; Blotting, Western ; Cell Shape ; Cells, Cultured ; Cytoskeleton ; metabolism ; Hela Cells ; pathology ; Histamine ; metabolism ; Humans ; Immunoenzyme Techniques ; Microfilaments ; metabolism ; Microtubules ; metabolism ; Mitosis ; physiology ; Mitotic Spindle Apparatus ; metabolism ; RNA Interference ; Recombinant Proteins ; isolation & purification ; metabolism ; Tumor Markers, Biological ; antagonists & inhibitors ; genetics ; metabolism ; Xenopus laevis

Introduction

Translationally Controlled Tumor-associated Protein (TCTP), also known as p23, IgE-dependent histamine releasing factor (HRF), mortalin or fortilin, is a highly conserved protein, which is up-regulated in certain cancers (e.g. prostate cancer cells; 1) and cancerous cell lines (e.g. in colorectal cancer cell line Caco-2; 2). Reduced expression of TCTP in cancerous cell lines reverts the transformed phenotype (3 ,4) whereas overexpression protects from apoptosis (5 –7). Its recent identification as a partner of Chfr, the key component of the early mitotic prophase checkpoint, increased again the interest in a potential role of TCTP in cancer etiology (8).

TCTP was initially identified as a growth-related protein on the basis of its translationally-dependent regulation of expression in mouse ascetic tumor and erythroleukemic cells (9 ,10). It is implicated in a broad diversity of intracellular functions as a stimulator of cell proliferation, growth, survival and stress responses (see Ref. 11). TCTP shares structural features with Rab-binding proteins from the Mss4/Dss4 family (GFCs), leading to the suggestion that TCTP could be a chaperone (12). Besides certain cancerous cells, TCTP is particularly abundant in highly proliferating cells, e.g. in spermatogonia of fetal rat testis and neonatal as well as in adult human testis (13). In Drosophila melanogaster TCTP controls cell growth and the rate of proliferation by regulating dRheb GTPase (14). Mouse TCTP gene inactivation is embryonic lethal, however, fibroblasts derived from TCTP −/− embryos apparently proliferate at a wild-type rate (15). This indicated that TCTP is not essential for cell viability (at least in fibroblasts), but may be involved in essential developmental processes in the mouse. TCTP is also a well known calcium-binding protein (1 ,16 ,17).

Mechanisms by which TCTP is implicated in so different intracellular functions remain elusive, except for a recently described role as a transcription factor regulating oct4 and nanog genes expression (18). The activity of TCTP as transcription factor activating the pluripotency genes oct4 and nanog (18) together with abundance of TCTP in highly proliferating cells makes this protein a potential candidate for a regulator of early development and stem cells proliferation. Indeed, a phosphorylated form of TCTP affected the reprogramming of nuclei in bovine nuclear transplant experiments and the rate of successfully cloned calves increased when this form of TCTP was enriched in oocytes (19). This effect of TCTP may depend on its activity as a genetic regulator, either as a transcription factor or a regulator of translation as it was reported to interact with elongation factor-1 delta (20).

Given that TCTP also resides in the cytoplasm and is associated with the cytoskeleton, it is likely to have non-genomic, cytoskeleton-mediated cellular functions. Several independent observations have led to a suggestion that TCTP interacts with microtubules (MTs). TCTP has been reported to colocalize with microtubules in vivo and could be purified in a complex with tubulin and MTs, with a potential MT-binding domain identified in the N-terminal part of the protein (21). Yeast mutants lacking TCTP are hypersensitive to the MT inhibitor benomyl providing a genetic link between TCTP and MT function (22). Consistent with this, in mouse oocytes and embryos, antibodies raised against TCTP decorate the mitotic spindle (23), while phosphorylation of TCTP by a key cell cycle-regulating kinase Plk1 has been implicated in destabilizing MTs (24). These various observations are suggestive of a close relationship between TCTP and the MT cytoskeleton, which may be important for regulation of cell cycle events, proliferation and therefore also for tumorigenesis.

Here we have examined in greater detail the association of TCTP with the cytoskeleton in Xenopus XL2 and human HeLa cells as well as in Xenopus oocytes and embryos cell-free extracts. The main goal was to define the cytoplasmic as opposed to transcriptional roles of this protein. Our data indicate that TCTP association with MTs is qualitatively different from that of conventional MT-associated proteins (MAPs) and is also tightly associated in a MT-independent manner with spindle poles in mitosis. Our major finding is that TCTP associates selectively with certain F-actin structures. Functional studies further indicate that TCTP is involved in regulating cell shape both during interphase and mitosis, probably via complex interactions with both the actin and MT cytoskeleton. Our study sheds new light on a plausible cytoskeleton-related role of TCTP in carcinogenesis.

Materials and methods

Tissue culture cells

The XL2 cell line was cultured in L-15 medium supplemented with 10 % fetal calf serum (FCS; full medium) and incubated at 25°C in air. HeLa cells were maintained in Dulbecco's modified Eagle's medium supplemented with 10 % fetal calf serum (FCS) and incubated at 37°C in 5 % CO_2 . Media were supplemented with penicillin (100 Units/ml) and streptomycin (100 mg/ml).

Immunocytochemistry of tissue culture cells

HeLa cells seeded on glass coverslips were fixed in 75 % methanol, 3.7 % formaldehyde, 0.5x PBS or in 3.7 % paraformaldehyde in 1x PBS for 10 min at room temperature and permeabilized with 0.1% Triton X100 in PBS for 5 min. DNA was visualized using DAPI. Polyclonal antibodies against Xl TCTP (raised in our laboratory) and against Hs TCTP (Santa-Cruz) were used at the dilution of 1:1000 and 1:100 respectively with overnight incubations at 4°C. Anti-β-tubulin (Sigma) and anti-α tubulin (Euromedex) were diluted 1:200. Purified anti-c-myc antibody (Sigma) was diluted 1:100. Secondary antibodies (FITC and RITC-conjugated, 1:1000 dilution; Molecular Probes) were incubated for 1 hr at room temperature. F-actin was detected with 2 units/ml of rhodamin-conjugated phalloidin (Molecular Probes). Coverslips were mounted in Vectashield and examined using a Leica DMRXA2 fluorescence microscope or Leica Confocal SP2 microscope. Photographs were taken using a black and white COOLsnap ES camera (Roper Scientific) and images were processed using Metamorph software (Universal Imaging).

Cell transfection

For transfection of XL2 cells with plasmids encoding Xenopus Myc-TCTP, 5×10^5 cells were plated on glass coverslips in a 12-well plate. Cells were transfected with 0.5 μg of plasmid DNA using FuGENE 6 Transfection Reagent (ROCHE) following the manufacturer's instructions.

Cell-free extracts and in vitro spindle assembly

Cytostatic factor-arrested extracts (CSF-extracts) were prepared as described (25). For in vitro spindle assembly, 0.5 μl of rhodamine-labeled bovine brain tubulin (Cytoskeleton) was added at 0.2 mg/ml and 2 μl of sperm heads at a concentration of ~1000 nuclei/μl added to 50 μl of the extract and incubated for 60–90 min at 21°C. Aliquots of extracts containing spindles (2–3 μl) were placed on a slide, covered with a coverslip, pressed with a finger, immediately fixed in liquid nitrogen, washed with PBS and processed for immunofluorescence (crude spindles). In vitro assembled spindles (15 μl of CSF-extract) were pre-fixed in 1 ml BRB80 buffer (80 mM K-Pipes, pH 6.8, 1 mM EGTA, 1 mM $MgCl_2$) containing 30 % glycerol, 1 % paraformaldehyde, and 0.5 % Triton X-100, and centrifuged (2300 × g, 30 min at room temperature) through a 40 % glycerol cushion in BRB80 onto glass coverslips in 12-wells plate. Spindles were fixed by adding 1 ml cold methanol (−20°C) for 10 min at room temperature (isolated spindles). Then fixed spindles were processed for immunocytochemistry.

Western blot

Protein samples were subjected to electrophoresis on 9 to 12.5 % SDS-PAGE gels (26). Separated proteins were transferred to nitrocellulose membranes (Hybond C, Amersham Biosciences) and probed with primary antibodies either against TCTP, c-myc, α-tubulin, Eg5 (gift from Jean-Pierre Tassan, Rennes) or tropomyosin (gift from Serge Hardy, Rennes). Antigen–antibody complexes were revealed

using alkaline phosphatase conjugated anti-rabbit or anti-mouse secondary antibodies (diluted 1:20,000) in combination with Enhanced Chemifluorescence reagent (ECF; Amersham Biosciences). Signal quantification was performed using ImageQuant 5.2 software (Amersham Biosciences).

Production and purification of recombinant XlTCTP wild-type and truncated proteins

To express Xenopus laevis TCTP, the 519-bp coding sequence was amplified by PCR from Xenopus egg cDNA with appropriate oligonucleotides including a BamHI (5′-end primer) and a HindIII (3′-end primer) restriction site and cloned into pGEM-T vector (Promega). Analysis of the sequence of the PCR product confirmed it coded for a 172-aa protein 100% identical to Xl TCTP (Tpt1-prov protein: GenBank accession number AAH43811). A cDNA coding for a truncated version of Xl TCTP lacking the MAP1B domain (TCTP Δ_{MAP1B} = aminoacids 1-81+122–172) was also constructed. Both TCTP cDNAs were then cut with BamHI and HindIII restriction enzymes and ligated in the corresponding site of the expression vector pQE30 (Qiagen). The resulting plasmids were transformed into XL1b E. coli bacteria (Novagen) which were then able to produce 6xHis-tagged Xl TCTP wt and ΔMAP1B upon addition of IPTG (isopropyl-b-D-thiogalactopyranoside). Both recombinant proteins were purified under denaturing conditions by affinity chromatography on cobalt resin (Talon™; Clontech), renatured by dialysis against PBS containing decreasing amounts of urea and finally concentrated by centrifugation using a Microsep™ device (molecular weight 10K cutoff; PALL). The full-length 6xHis-tagged Xl TCTP was used to raise rabbit polyclonal antibody against Xenopus TCTP (Charles River Laboratories) and both proteins were also used in various assays.

In vitro microtubule self-assembly and disassembly

Tubulin was purified from pig brain as described (27). The purity of tubulin was checked by electrophoresis, and the absence of endogenous TCTP confirmed by Western blotting. 50 μM samples of tubulin were incubated for 10 min at 4°C with 1 mM GTP in BRB80 buffer. Microtubule assembly was induced at 37°C and monitored turbidimetrically at 350 nm. After 35 min, microtubule depolymerization was triggered by lowering the temperature to 4°C. To study the effect of full-length and truncated TCTP (TCTP$^{\Delta MAP1B}$) on microtubule assembly/disassembly, increasing concentrations of the purified proteins were added to tubulin at 4°C before starting the assembly process. As positive controls (data not show), we checked that the N terminal fragment of CLIP-170 named H2 (28 ,29) and EB1 strongly stimulated microtubule assembly as reported previously (30 ,31).

In vitro assays for XlTCTP binding to microtubules and F-actin

Taxol-stabilized microtubules were incubated for 15 min at 37°C with TCTP or CLIP-170 (H2) in BRB80 buffer (80 mM Pipes, 1 mM $MgCl_2$, and 1 mM EGTA). Microtubules were sedimented by centrifugation at 80,000×g for 30 min at 37°C. G-actin (monomeric actin) from rabbit skeletal muscles in G-buffer (5mM Tris-HCl pH 7.8, 0.1 mM $CaCl_2$, 0.2 mM ATP, 1mM DTT, 0.01 % NaN_3) was polymerized into F-actin (filamentous actin) by addition of 100 mM KCl, 1mM $MgCl_2$ and 0.2 mM EGTA. F-actin was incubated for 15 min at room temperature with TCTP in buffer F (5mM Tris-HCl pH 7.8, 100mM KCl, 1mM $MgCl_2$, 0.1 mM $CaCl_2$, 0.2 mM ATP, 1mM DTT, 0.01 % NaN_3). The filaments were collected by centrifugation at 90,000 × g for 30 min at 20°C. In both assays, proteins in the supernatants and pellets were solubilized in SDS sample buffer and analyzed after SDS-PAGE and silver staining or Western blotting.

RNA interference

Human and Xenopus TCTP siRNAs were purchased from Eurogentec. A single Xenopus TCTP siRNA with the following nucleotide sequence 5′-CCAAGGACUCUUACAAGAA-3′ and three Human TCTP siRNAs with sequences: A: 5′ -CUCGCUCAUUGGUGGAAAU-3′; B: 5′-GGACAGAAGGUAACAUUGA-3′; C: 5′-GGUACCGAAAGCACAGUAA-3′ were used. The “universal negative control” siRNA (OR-0030-neg05) designed by Eurogentec was also used. Cells were transfected with oligonucleotides using HiPerFect Transfection Reagent (Qiagen) following the manufacturer’s instructions (in 12-wells plate: Xenopus siRNA at 50 nM final with 9μl HiPerFect; Human siRNAs at 5 nM final with 3μl HiPerFect).

Results

TCTP partially colocalizes with the MT cytoskeleton in XL2 cells

TCTP was previously identified as a putative cell cycle-dependent MT-associated protein in monkey COS cells on the basis of immunofluorescence localization and by detection of the affinity binding to MTs and tubulin (21). To investigate the cytoskeletal roles of this protein we first examined the intracellular localization of endogenous and exogenous (Myc-tagged) Xl TCTP in Xenopus XL2 cells. The specificity of the antibody used in this study was confirmed by Western blotting (Fig. 1A, a,b). Immunofluorescence and transfection experiments revealed equivalent patterns of intracellular TCTP localization (Fig. 1A, c–g), conforming to the previous description (21). In interphase cells (methanol/formaldehyde fixation), TCTP formed a fibrous, MT-like network, while in mitotic cells it accumulated in the spindle as well as in granular or fibrous structures in the cytoplasm (Fig. 1A, c–g) which is MT-free during mitosis. Similarly as in monkey COS cells, TCTP was not detected in the midbody (Fig. 1A, d ; tubulin staining in the inset)(21). Similar pattern of TCTP was also shown recently in XL2 cells (8). Careful examination of cells co-stained with β-tubulin, however, revealed small but consistent

differences between the TCTP network and the MT network in interphase cells (Fig. 1B). Many instances of individual fibers stained exclusively with anti-β-tubulin or exclusively with anti-TCTP were detected, especially in thin and flattened areas at the edges of cells (Fig. 1B, a–d). In cells treated with colchicine to cause partial disassembly of the MT network, differences in the distributions of TCTP and β-tubulin became obvious also in the central region of interphase cells (Fig. 1B, e,f). Prolonged colchicine treatment resulted in total disassembly of both MT and TCTP networks (data not shown) suggesting that despite local differences, the two networks are related and that the TCTP network is dependent on the integrity of MTs. The pattern of TCTP fibers bears some resemblance to that described for vimentin intermediate filaments. However, double immunofluorescence for TCTP and vimentin showed that these networks are clearly distinct (Suppl. Mat. Fig. 1). A strong granular signal of anti-TCTP staining was also present in the cytoplasm (particularly well visible in the cytoplasm of mitotic cells, Fig. 1A,c), suggesting that a significant fraction of TCTP is either soluble or associated with a cytoplasmic lattice, consistent with the abundance of the protein apparent in Western blots. We conclude that TCTP is present in XL2 cells cytoplasm as MT-like fibrous network and cytosolic pool. Although the fibrous TCTP localization is highly reminiscent of the MT network the colocalization is not strict and TCTP-free MTs as well as tubulin-free TCTP-positive fibers co-exist within the cell.

TCTP associates strongly with mitotic spindle poles

To examine in detail TCTP localization within the spindle we used “CSF” cytoplasmic extract (metaphase-arrested oocytes) in which spindles were assembled around sperm nuclei and visualized using rhodamine-labeled tubulin. Immunofluorescence of spindles frozen within thin layer of crude cell-free extract (Fig. 2A , top panel) confirmed enrichment of TCTP in the spindles, as seen in XL2 cells (Fig. 1A, c,f). However, the fibrous, not linked to MTs organization of TCTP staining was restricted to the cytoplasm (Fig. 2A , top panel; MT-free cytoplasm around spindles in corners of the fig. 2A, b and d). Moreover, the intense staining of the spindles was relatively homogeneous compared to the tubulin staining (Fig. 2A , top panel; black arrows show tubulin-positive fibers, white arrows show the absence of TCTP fibers at the corresponding sites within the spindle). In the spindle, TCTP thus did not show details of features of distribution predicted for a MAP. Unexpectedly, in vitro assembled spindles isolated by centrifugation through a glycerol cushion showed a major loss of anti-TCTP staining, with some TCTP signal retained selectively at the spindle poles (Fig. 2A, f). The residual TCTP remaining within such spindles was again neither fibrous nor colocalized with MTs. These results confirm that TCTP is enriched in mitotic spindles, but indicate that it is not linked directly to MTs, with a strong association only at the spindle poles.

Neither TCTP nor TCTP$^{\Delta MAP1B}$ modify MTs assembly/disassembly in vitro

The results described above suggest that either TCTP is not associated directly with MTs or that this association differs significantly from that of other MAPs. Nevertheless, TCTP possesses a domain resembling the MT-binding domain of MAP1B (21). To clarify the microtubule-interacting properties of TCTP we produced a recombinant His-tagged mutant protein, TCTP$^{\Delta MAP1B}$, lacking the MAP1B-like domain (amino-acids 82 to 121) and compared its activity with intact recombinant protein in in vitro MT assembly/disassembly assays. In contrast with the stimulatory effects of an N-terminal fragment of CLIP170 (H2) or EB1 protein observed in the same laboratory (data not shown; 30,31), inclusion of either TCTP or TCTP$^{\Delta MAP1B}$ in the assays did not significantly affect rates of MT polymerization at 37°C or of MT disassembly at 4°C (Fig. 2B). We also examined the localization of TCTP$^{\Delta MAP1B}$ after expression in XL2 cells, and found that this truncated form became distributed very similarly to intact TCTP: cytoplasmic staining in interphase and both cytoplasmic and spindle staining in mitosis (Fig. 2C). We conclude from these studies that neither intact TCTP nor a form lacking the putative MT-binding domain modifies MT dynamics, and that this domain is not required for the MT-like distribution of TCTP in cells.

TCTP has no affinity for taxol-stabilized MTs in vitro

We next investigated the affinity of TCTP for in vitro assembled taxol-stabilized MTs. When recombinant 6xHis-tagged Xl TCTP was incubated alone at 37°C in the MT-stabilization buffer and then spun down, approximately half of it was pelleted (Fig. 3A) likely reflecting the capacity of TCTP to oligomerize (32). Surprisingly, even high amounts of taxol-stabilized MTs did not significantly increase the quantity of TCTP in the pellet (Fig. 3B , TCTP in the middle panel). Under the same conditions, the H2 N-terminal fragment of CLIP-170 clearly interacted with microtubules (Fig. 3B , H2 in the bottom panel). Thus, the soluble fraction of 6xHis-tagged Xl TCTP lacks detectable affinity for MTs in the co-sedimentation assay. Being aware that the recombinant protein could be misfolded and thus could not reflect the properties of the native protein we carefully analyzed the affinity of MTs with a TCTP protein expressed in conditions assuring its functionality. Rigorously equivalent results were obtained in a co-sedimentation assay with untagged as well as Myc-tagged Xl TCTP translated in rabbit reticulocyte lysates. (Fig. 3C). This shows that the absence of detectable TCTP/MT interactions was neither related to the bacterial origin nor to the purification procedure of the recombinant protein shown in Fig. 3B , but that the properly folded TCTP protein indeed has no detectable affinity for MTs in our assay.

To test for interactions between native TCTP and MTs in the presence of endogenous cytoplasmic proteins we applied a co-sedimentation assay using Xenopus egg cytoplasmic extracts (Fig. 3D). Taxol-stabilized MTs were mixed with either interphase or M-phase (CSF) extracts diluted in appropriate buffer, incubated and spun down. The ratio of distribution of endogenous TCTP in the

supernatant and pellets was compared. Under these conditions, the kinesin-related Eg5 protein, known to interact with MTs (33), was shown to become enriched in the MT pellet as expected (Fig. 3D , bottom: pelleted MTs appear saturated with endogenous Eg5 and moderate increase is observed). The amount of endogenous TCTP found within the fraction along with MTs did not, however, increase in either type of cell-free extract (Fig. 3D). We conclude that neither bacterially expressed nor native TCTP behave as MT-binding proteins under these assay conditions.

Finally, to modulate the quantity of MTs and eventual proportions of TCTP in supernatant and pellet fractions we added into interphase and M-phase extracts either a low dose of nocodazole or taxol to respectively decrease or increase the volume (number and length) of MTs in extracts and the volume of the pellet. As expected, the amount of MTs in the insoluble fraction (P) diminished slightly in the presence of nocodazole and clearly increased when taxol was added (Fig. 3E , right). However, the quantities of TCTP in the pellet fraction rigorously did not change at all (Fig. 3E , left). Thus, the endogenous TCTP present in Xenopus laevis interphase and M-phase-arrested cell-free extracts lacks an affinity for MTs which could be detected in co-sedimentation assay.

TCTP associates with actin-rich structures in XL2 cells

Careful examination of anti-TCTP immunofluorescence and of Myc-tagged exogenous TCTP in paraformaldehyde fixed XL2 cells revealed a distinctive discrete pattern at the cell border in spreading cells (Fig. 4A). Double staining of TCTP and F-actin (using rhodamine-phalloidin) in these cells revealed a significant colocalization between the two proteins in these cellular regions (Fig. 4B). TCTP strongly colocalized with F-actin at the leading edge of peripheral ruffles. In addition, TCTP colocalized with curly actin-rich fibers proximal to the lamellipodia and those resembling dorsal ruffles (Fig. 4B). In contrast, stress fibers, the most solid and abundant F-actin structures were not stained with TCTP antibody (data not shown). Actin-rich peripheral and dorsal ruffles were visible also in XL2 cells transfected with Myc-TCTP, and in spreading HeLa cells (data not shown). Cytochalasin D treatment depolymerises F-actin and provokes, as a side effect, formation of actin-rich residual foci within cells. TCTP clearly colocalized with these cytochalasin-induced actin foci (Fig. 4B , bottom) indicating that TCTP can accompany actin-rich structures upon their rearrangement. These data suggest that TCTP associates with F-actin structures at the periphery of spreading cells and with actin foci upon cytochalasin D treatment. The absence of TCTP in stress fibers suggested that this association is under complex regulation and/or may be indirect.

TCTP associates with F-actin in cell-free extracts

As TCTP colocalizes with certain actin structures in vivo, we tested potential interactions between F-actin and TCTP using an in vitro co-sedimentation assay (34). The sedimentation of recombinant 6His-tagged Xl TCTP did not increase in the presence of actin filaments (Fig. 4C). Similar results were obtained when F-actin was incubated with a reticulocyte lysate containing in vitro translated Xl TCTP or Myc-Xl TCTP (data not shown). However, when actin filaments were incubated in egg extracts, a significant co-sedimentation of endogenous TCTP with F-actin was observed (Fig. 4D). The proportion of TCTP found in the pellet was comparable to that of tropomyosin, a well-characterized F-actin binding protein (Fig. 4D , bottom). The exclusion from the actin pellet of proteins detected non-specifically by the anti-tropomyosin antibody additionally confirmed the specificity of the assay for F-actin binding proteins. The co-sedimentation of endogenous TCTP with F-actin in egg extracts but not of recombinant or reticulocyte-translated TCTP with purified F-actin indicates that this interaction is indirect, and/or requires some post-translational modification(s) of either TCTP or actin.

TCTP knockdown changes the shape of XL2 and HeLa cells

To analyse the role of TCTP in vivo we used siRNA to reduce levels of this protein in XL2 cells. In cells treated with TCTP siRNA oligonucleotides, TCTP levels were reduced by about 50% (Fig. 5A). Similar difficulty to knock down TCTP in XL2 cells was reported recently (8). The most striking effect of TCTP knockdown was a drastic change in the shape of the cells, which became elongated with characteristic perpendicular protrusions, loosing the flatness of the cell body such that nuclei could not be distinguished in phase contrast images as they easily could be in flattened control cells (Fig. 5A , right). Moreover, the cells seem to change their contact properties. While control XL2 cells grow in “islands” of well attached flattened cells, those in which TCTP was down regulated showed only a limited area of cell-to-cell contact and despite that they did not tend to form “islands” (Fig. 5A , right). Since XL2 cells are resistant to transfection and their RNAi is quite inefficient (8), we performed highly more efficient RNAi experiments in HeLa cells, using three different siRNA oligonucleotides directed towards human TCTP. All three siRNAs provoked significant reductions in TCTP levels as shown by Western blotting (Fig. 5B). Besides well known effects of TCTP knock down as slowed down proliferation and increased apoptosis, the most dramatic phenotypic effect was again a drastic change of cell shape that became elongated with long protrusions (Fig. 5B). The same elongated phenotype was equally visible in dispersed as in closely apposed cells (compare Fig. 5B with 6B,C,D) showing that the change in cells shape is not due to cells isolation following slowed down proliferation and increased apoptosis. HeLa cells do not adhere closely one to another as XL2 cells do, and there was no obvious change in their cell-to-cell contact properties following RNAi (compare dispersed cells in Fig. 5B and more closely apposed ones in Fig. 6B). In highly elongated HeLa cells with decreased TCTP levels, the MT cytoskeleton was disorganized and MTs formed dense cables (Fig. 5B). Spreading cells disappeared upon TCTP knockdown conditions and lamellipodia in which TCTP colocalized with actin were absent (Fig. 6B). The cortical accumulation of actin and numerous fibers perpendicular to the cells axis were present in such highly elongated cells indication reorganization of actin cytoskeleton (Fig. 6B).

Interestingly, addition of nocodazole restored the cell shape abnormalities induced by siRNA in interphase cells (Fig. 6C), demonstrating that the change is MT-dependent. The strong TCTP staining in the spindles of control HeLa cells disappeared (Fig. 6A second and third row) or diminished dramatically (Fig. 6A , forth and bottom row) following RNAi. Long cytoplasmic protrusions were occasionally found also during mitosis in siRNA-treated cells (Fig. 6A,D) in clear contrast to perfectly round-up control cells (Fig. 6A , control). These protrusions were always positioned at a single or two ends of the long axis of elongated cells. In the first case, cytokinesis created cells with different sizes (Fig. 6D). Thus, TCTP depletion has dramatic consequences on cell shape both during interphase and mitosis, exerting effects on both actin and MT cytoskeletons. Mitotic spindles in cells with knocked down TCTP were indistinguishable from controls when observed with anti-tubulin immunofluorescence (Fig. 5B , oligo A, MTs).

Discussion

In this paper we have examined in detail the relationship between TCTP and the cytoskeleton. Our results have demonstrated for the first time that TCTP associates with certain F-actin structures and that this protein is involved in shaping of Xenopus XL2 and human HeLa cells. We have also shown that despite striking similarities between TCTP and MT networks they are not completely super-imposable, and that TCTP has no affinity for taxol-stabilized MTs. Gachet and colleagues (21) were first to implicate TCTP with microtubules by showing that TCTP can be immunoprecipitated with anti-tubulin antibodies and that in COS cells TCTP co-aligns with microtubules. Rinnerthaler and colleagues (22) suggested that TCTP interacts with microtubules based on the hypersensitivity of TCTP knockout cells to benomyl. However, in our in vitro experiments we could neither confirm the affinity of both recombinant and native TCTP to MTs nor detect any influence of TCTP on MT dynamics. Furthermore, in an organism extremely rich in microtubules, the protist Tetrahymena thermophila , GFP-tagged TCTP does not localize to MTs and a genetic knockout of Tt TCTP gene does not influence the MT cytoskeleton (D. Wloga and J. Gaertig, personal communication). Finally, the abundant TCTP in mitotic spindles does not colocalize with discrete MT fibers but is rather associated with non-fibrous spindle elements, and also strongly associates with the spindle poles (this paper). Taken together these data enable us to refute earlier claims of a direct association of TCTP with MTs (21). Nevertheless, in line with the conclusions of previous research (21 ,22 ,24), we did find evidences for a relationship between TCTP and MTs, the changes in the shape of siRNA-treated and TCTP knocked down HeLa cells being found to be MT-dependent (this paper). Given our lack or evidence for direct binding, the effect of TCTP on the MT cytoskeleton is probably indirect.

The MT-like organization of TCTP in a form of network is intriguing. The absence of TCTP on certain MTs and the absence of tubulin in certain TCTP-stained fibers, as well as the increase of tubulin-negative TCTP fibers upon colchicine treatment, suggest that TCTP may associate with MTs following assembly and remain transiently in the place of individual MTs following their disassembly. Such behavior has been reported previously for the 7/13 antigen in mouse oocytes (35). The protein reacting with 7/13 antibody is a component of calcium transport system and it is organized in fibers which trace disassembled MTs, and guide newly forming ones (35). Interestingly TCTP is also a calcium-binding protein (1 ,16 ,17) and could thus also be involved in MT guiding.

We show in the current paper that TCTP is a mitotic spindle protein without detectable affinity for MTs. The pattern of non-fibrous staining and the disappearance of TCTP from isolated spindles suggest that the majority of TCTP is either a spindle matrix protein or associates with spindle structures other than MTs. The role of the spindle matrix is still a matter of debate. However, the recent finding that the nuclear intermediate filament protein lamin B contributes to the spindle matrix and plays an important role in spindle morphogenesis strengthened speculation that such matrix could be more important for appropriate cell division than previously thought (36 ,37). As TCTP is particularly concentrated in the spindle, forms lattice in the cytoplasm (as shown in Xenopus cell-free extract; Fig. 2A in this paper) and is capable of oligomerization (32), it is a good candidate to participate in a mitotic spindle scaffold. We cannot exclude however, that TCTP is associated with actin present within spindle or with other spindle components. Persistence of TCTP on the spindle poles after spindle isolation on a glycerol cushion (this paper) could suggest that either it is particularly tightly packed on the spindle poles or forms an integral part of centrosomes. These aspects need further analysis.

We show that TCTP colocalizes with actin structures at the leading edge of lamellipodia-like cells and in actin bundles of peripheral and dorsal ruffles at the rear of the lamellipodia (e.g.38–40). In agreement with our observations, endogenous TCTP associates with actin filaments in a co-sedimentation assay in the presence of cell-free Xenopus egg extracts. To our knowledge this is the first indication of actin-binding capacity for TCTP, although this binding may require either a post-translational modification and/or additional adaptors to bind since no interaction was observed in the absence of egg extracts. A potential adaptor is the light chain of myosin, a well-known actin filament binding protein which has been described as a TCTP binding protein (41). Association of TCTP with actin-containing structures, perhaps via myosin, could explain why RNAi depletion of TCTP dramatically affected both the shape and the cytoskeleton organization of tissue culture cells. The actin cytoskeleton plays a critical role in maintaining cell shape, so it is tempting to propose that the ability of TCTP to bind actin filaments is related to its role in cell shaping.

Our results showing that the change of shape of HeLa cells under siRNA treatment is MT-dependent do not contradict active interactions between TCTP and actin structures. Moreover, TCTP overexpression also induces changes in the MT cytoskeleton, with the formation of MT cable attributed to the supposed action of the protein as a MAP (21). Such MT reorganizations could, however, result

indirectly from perturbations in other cytoskeletal systems, including F-actin structures positioned perpendicularly to the axis of elongated cells with reduced TCTP (this paper, Fig. 6B). Even bona fide MAPs, like MAP1B, have the capacity to bind both MTs and actin (42 ; see Ref. 43). Partial colocalization of TCTP with MTs and actin resembles localization of MT- and actin-binding protein Mip-90 in human fibroblasts (44), with notable exception of stress fibers stained with anti-Mip-90 antibody, but not with anti-TCTP. Cell shaping is a complex phenomenon in which all cytoskeletal elements are implicated and interact one with another (see Refs 45 ,46). Thus F-actin-binding of TCTP remains fully compatible with the role of this protein in MT-dependent shaping of tissue culture cells. This conclusion is strengthened by our observation that upon TCTP knock down changes in cell shape occur also during mitosis. Indeed, the long protrusions in TCTP knocked down HeLa cells may persist in mitosis resulting in unequally sized daughter cells. Since the cytoplasmic network of MTs disassembles at the beginning of the M-phase in control and RNAi TCTP HeLa cells (Fig. 5B ; MTs) the protrusions are also devoid of MTs. Interestingly, the protrusions observed in mitotic HeLa cells generally were oriented along the axis of cell division (see Fig. 6A and D). This may coincide with the persistence of the strongest retraction fibers during mitosis (47). The occasional character of such phenotype suggests that it concerns only extremely strong retraction fibers. Apparently, in cells with low TCTP level, both actin and MT cytoskeleton escapes from normal control. Cytoskeleton-linked functions of TCTP could play important roles particularly in malignancy as cells flexibility and motility changes in malignant cells. TCTP is a good candidate to regulate the two cytoskeleton networks by integrating their organization and coordinating these two cytoskeletal elements during cell shaping.

In summary, this study provides the first evidence that: i) TCTP interacts with F-actin, ii) its relationship with MTs is less direct than thought so far, iii) this protein regulates cell shape in a cytoskeleton-dependent manner. Further analysis of TCTP interactions both with MTs and F-actin should give us more insights into the role of TCTP in normal and cancer cells.

Ackowledgements:

Funding

ARC (4900) and Ligue Contre le Cancer (Comité d'Ille-et-Vilaine et de Vendée) to J.Z.K.

We thank Dorota Wloga and Jacek Gaertig (University of Georgia, Athens) who shared with us unpublished observations concerning Tetrahymena thermophila TCTP knock-out, exchanged information, discussed and helped us to prepare this manuscript including English correction. We wish to thank Stephanie Dutertre (IFR 140 GFAS) for her technical assistance with microscopy work. We are grateful to Evelyn Houliston (Observatoire de Villefranche sur Mer) and William Forrester (Novartis Institutes for Biomedical Research) for fruitful discussions, reading the manuscript and valuable English corrections.

Abbreviations

TCTP : Translationally Controlled Tumor-associated Protein
MT : microtubule
MAP : microtubule-associated protein
HRF : histamine releasing factor
siRNA : small interfering RNA
RNAi : RNA interference

References:

- 1 . Arcuri F , Papa S , Carducci A , Romagnoli R , Liberatori S , Riparbelli MG , Sanchez JC , Tosi P , del Vecchio MT . 2004 ; Translationally controlled tumor protein (TCTP) in the human prostate and prostate cancer cells: expression, distribution, and calcium binding activity . Prostate . 60 : 130 - 140
- 2 . Stierum R , Gaspari M , Dommels Y , Ouatas T , Pluk H , Jespersen S , Vogels J , Verhoeckx K , Groten J , van Ommen B . 2003 ; Proteome analysis reveals novel proteins associated with proliferation and differentiation of the colorectal cancer cell line Caco-2 . Biochim Biophys Acta . 1650 : 73 - 91
- 3 . Tuynder M , Susini L , Prieur S , Besse S , Fiucci G , Amson R , Telerman A . 2002 ; Biological models and genes of tumor reversion: cellular reprogramming through tpt1/TCTP and SIAH-1 . Proc Natl Acad Sci USA . 99 : 14976 - 14981
- 4 . Tuynder M , Fiucci G , Prieur S , Lespagnol A , Geant A , Beaucourt S , Duflaut D , Besse S , Susini L , Cavarelli J , Moras D , Amson R , Telerman A . 2004 ; Translationally controlled tumor protein is a target of tumor reversion . Proc Natl Acad Sci USA . 101 : 15364 - 15369
- 5 . Li F , Zhang D , Fujise K . 2001 ; Characterization of fortilin, a novel antiapoptotic protein . J Biol Chem . 276 : 47542 - 47549
- 6 . Liu H , Peng HW , Cheng YS , Yuan HS , Yang-Yen HF . 2005 ; Stabilization and enhancement of the antiapoptotic activity of mcl-1 by TCTP . Mol Cell Biol . 25 : 3117 - 3126
- 7 . Yang Y , Yang F , Xiong Z , Yan Y , Wang X , Nishino M , Mirkovic D , Nguyen J , Wang H , Yang XF . 2005 ; An N-terminal region of translationally controlled tumor protein is required for its antiapoptotic activity . Oncogene . 24 : 4778 - 4788
- 8 . Burgess A , Labbé JC , Vigneron S , Bonneaud N , Strub JM , Van Dorsselaer A , Lorca T , Castro A . 2008 ; Chfr interacts and colocalizes with TCTP to the mitotic spindle . Oncogene . (in press)
- 9 . Yenofsky R , Cereghini S , Krowczynska A , Brawerman G . 1983 ; Regulation of mRNA utilization in mouse erythroleukemia cells induced to differentiate by exposure to dimethyl sulfoxide . Mol Cell Biol . 3 : 1197 - 1203
- 10 . Chitpatima ST , Makrides S , Bandyopadhyay R , Brawerman G . 1988 ; Nucleotide sequence of a major messenger RNA for a 21 kilodalton polypeptide that is under translational control in mouse tumor cells . Nucleic Acids Res . 16 : 2350 -
- 11 . Bommer UA , Thiele BJ . 2004 ; The translationally controlled tumour protein (TCTP) . Int J Biochem Cell Biol . 36 : 379 - 385
- 12 . Thaw P , Baxter NJ , Hounslow AM , Price C , Waltho JP , Craven CJ . 2001 ; Structure of TCTP reveals unexpected relationship with guanine nucleotide-free chaperones . Nat Struct Biol . 8 : 701 - 704
- 13 . Guillaume E , Pineau C , Evrard B , Dupaix A , Moertz E , Sanchez JC , Hochstrasser DF , Jégou B . 2001 ; Cellular distribution of translationally controlled tumor protein in rat and human testes . Proteomics . 1 : 880 - 889

- 14 . Hsu YC , Chern JJ , Cai Y , Liu M , Choi KW . 2007 ; Drosophila TCTP is essential for growth and proliferation through regulation of dRheb GTPase . Nature . 445 : 785 - 788
- 15 . Chen SH , Wu PS , Chou C , Yan YT , Liu H , Weng S , Yang-Yen H . 2007 ; A knockout mouse approach reveals that TCTP functions as an essential factor for cell proliferation and survival in a tissue- or cell type-specific manner . Mol Biol Cell . 18 : 2525 - 2532
- 16 . Arcuri F , Papa S , Meini A , Carducci A , Romagnoli R , Bianchi L , Riparbelli MG , Sanchez JC , Palmi M , Tosi P , Cintorino M . 2005 ; The translationally controlled tumor protein is a novel calcium binding protein of the human placenta and regulates calcium handling in trophoblast cells . Biol Reprod . 73 : 745 - 751
- 17 . Kim M , Jung Y , Lee K , Kim C . 2000 ; Identification of the calcium binding sites in translationally controlled tumour protein . Arch Pharma Res . 23 : 633 - 636
- 18 . Koziol MJ , Garrett N , Gurdon JB . 2007 ; Tpt1 activates transcription of oct4 and nanog in transplanted somatic nuclei . Curr Biol . 17 : 801 - 807
- 19 . Tani T , Shimada H , Kato Y , Tsunoda Y . 2007 ; Bovine Oocytes with the Potential to Reprogram Somatic Cell Nuclei Have a Unique 23-kDa Protein, Phosphorylated Transcriptionally Controlled Tumor Protein (TCTP) . Cloning Stem Cells . 9 : 267 - 280
- 20 . Langdon JM , Vonakis BM , MacDonald SM . 2004 ; Identification of the interaction between the human recombinant histamine releasing factor/translationally controlled tumor protein and elongation factor-1 delta (also known as elongation factor-1B beta) . Biochim Biophys Acta . 1688 : 232 - 236
- 21 . Gachet Y , Tournier S , Lee M , Lazaris-Karatzas A , Poulton T , Bommer UA . 1999 ; The growth-related, translationally controlled protein P23 has properties of a tubulin binding protein and associates transiently with microtubules during the cell cycle . J Cell Sci . 112 : 1257 - 1271
- 22 . Rinnerthaler M , Jarolim S , Heeren G , Palle E , Perju S , Klinger H , Bogengruber E , Madeo F , Braun RJ , Breitenbach-Koller L , Breitenbach M , Laun P . 2006 ; MMI1 (YKL056c, TMA19), the yeast orthologue of the translationally controlled tumor protein (TCTP) has apoptotic functions and interacts with both microtubules and mitochondria . Biochim Biophys Acta . 1757 : 631 - 638
- 23 . Miyara F , Han Z , Gao S , Vassena R , Latham KE . 2005 ; Non-equivalence of embryonic and somatic cell nuclei affecting spindle composition in clones . Dev Biol . 289 : 206 - 217
- 24 . Yarm FR . 2002 ; Plk phosphorylation regulates the microtubule-stabilizing protein TCTP . Mol Cell Biol . 22 : 6209 - 6221
- 25 . Murray AW . 1991 ; Cell cycle extracts . Methods Cell Biol . 36 : 581 - 605
- 26 . Laemmli UK . 1970 ; Cleavage of structural proteins during the assembly of the head of bacteriophage T4 . Nature . 227 : 680 - 685
- 27 . Ashford AJ , Andersen SLA , Hyman AA . 1998 ; Preparation of tubulin from bovine brain . Cell Biology a Laboratory Handbook . 2 : Academic Press ; San Diego 205 - 212
- 28 . Pierre P , Scheel J , Rickard JE , Kreis TE . 1992 ; CLIP-170 links endocytic vesicles to microtubules . Cell . 70 : 887 - 900
- 29 . Scheel J , Pierre P , Rickard JE , Diamantopoulos GS , Valetti C , van der Goot FG , Haner M , Aebi U , Kreis TE . 1999 ; Purification and analysis of authentic CLIP-170 and recombinant fragments . J Biol Chem . 274 : 25883 - 25891
- 30 . Arnal I , Heichette C , Diamantopoulos GS , Chrétien D . 2004 ; CLIP-170/tubulincurved oligomers coassemble at microtubule ends and promote rescues . Curr Biol . 14 : 2086 - 2095
- 31 . Vitré B , Coquelle FM , Heichette C , Garnier C , Chrétien D , Arnal I . 2008 ; EB1 regulates microtubule dynamics and tubulin sheet closure in vitro . Nat Cell Biol . 10 : 415 - 21
- 32 . Yoon T , Jung J , Kim M , Lee KM , Choi EC , Lee K . 2000 ; Identification of the self-interaction of rat TCTP/IgE-dependent histamine-releasing factor using yeast two-hybrid system . Arch Biochem Biophys . 384 : 379 - 82
- 33 . Sawin KE , LeGuellec K , Philippe M , Mitchison TJ . 1992 ; Mitotic spindle organization by a plus-end-directed microtubule motor . Nature . 359 : 480 - 482
- 34 . Laurent V , Loisel TP , Harbeck B , Wehman A , Grobe L , Jockusch BM , Wehland J , Gertler FB , Carlier MF . 1999 ; Role of proteins of the Ena/VASP family in actin-based motility of Listeria monocytogenes . J Cell Biol . 144 : 1245 - 1258
- 35 . de Pennart H , Cibert C , Petzelt C , Maro B . 1994 ; Microtubule tracks can be detected in mouse oocytes with an antibody directed against a calcium transporter . J Cell Sci . 107 : 1899 - 1908
- 36 . Tsai MY , Wang S , Heidinger JM , Shumaker DK , Adam SA , Goldman RD , Zheng Y . 2006 ; A mitotic lamin B matrix induced by RanGTP required for spindle assembly . Science . 311 : 1887 - 1893
- 37 . Zheng Y , Tsai MY . 2006 ; The mitotic spindle matrix: a fibro-membranous lamin connection . Cell Cycle . 5 : 2345 - 2347
- 38 . Krueger EW , Orth JD , Cao H , McNiven MA . 2003 ; A dynamin-cortactin-Arp2/3 complex mediates actin reorganization in growth factor-stimulated cells . Mol Biol Cell . 14 : 1085 - 1096
- 39 . Kurisu S , Suetsugu S , Yamazaki D , Yamaguchi H , Takenawa T . 2005 ; Rac-WAVE2 signaling is involved in the invasive and metastatic phenotypes of murine melanoma cells . Oncogene . 24 : 1309 - 1319
- 40 . Applewhite DA , Barzik M , Kojima S , Svitkina TM , Gertler FB , Borisy GG . 2007 ; Ena/VASP proteins have an anti-capping independent function in filopodia formation . Mol Biol Cell . 18 : 2579 - 2591
- 41 . Kim MJ , Jung J , Choi EC , Park HY , Lee K . 2001 ; Identification of the interaction between rat translationally controlled tumor protein/IgE-dependent histamine releasing factor and myosin light chain . J Biochem Mol Biol . 34 : 526 - 530
- 42 . Noiges R , Eichinger R , Kutschera W , Fischer I , Nemeth Z , Wiche G , Propst F . 2002 ; Microtubule-associated protein 1A (MAP1A) and MAP1B: light chains determine distinct functional properties . J Neurosci . 22 : 2106 - 2114
- 43 . Halpain S , Dehmelt L . 2006 ; The MAP1 family of microtubule-associated proteins . Genome Biol . 7 : 224 -
- 44 . González M , Cambiazo V , Maccioni RB . 1998 ; The interaction of Mip-90 with microtubules and actin filaments in human fibroblasts . Exp Cell Res . 239 : 243 - 253
- 45 . Théry M , Bornens M . 2006 ; Cell shape and cell division . Curr Opin Cell Biol . 18 : 648 - 657
- 46 . Basu R , Chang F . 2007 ; Shaping the actin cytoskeleton using microtubule tips . Curr Opin Cell Biol . 19 : 88 - 94
- 47 . Théry M , Jiménez-Dalmaroni A , Racine V , Bornens M , Jülicher F . 2007 ; Experimental and theoretical study of mitotic spindle orientation . Nature . 447 : 493 - 496

Fig. 1

TCTP and microtubules form similar, but not identical, networks in XL2 cells

(A) Western blotting showing specificity of the serum used to detect Xenopus laevis TCTP (a). Lanes: 1 and 1′ recombinant His-TCTP; 2 and 2′ XL2 cells extract, 3 and 3′ CSF extract made of Xenopus ovulated MII oocytes. Preimmune serum (b) used in 1/5000 concentration, the same as the immune serum shown in (a) delivers virtually no background. Therefore, we show here a WB with more concentrated (1:1000) preimunne serum (b) showing only traces of non specific bands. Immunofluorescence localization of endogenous TCTP (c and d in the top panel) and Myc-TCTP localization (f and g in the bottom panel) following expression in XL2 cells. In mitotic cells TCTP localizes to the division spindle as well as it forms a granular network in the cytoplasm (c; a single confocal section through metaphase cell). In interphase cells, TCTP forms dense cytoplasmic network similar to MTs (d). Midbody stained with anti-tubulin (white arrow in the inset) is however, free of TCTP (white arrow in d). Control staining with preimmune serum (e) shows the specificity of the immunofluorescence staining with the serum. Preimmune serum gives a faint background with no fibrous staining. Myc-TCTP was expressed and localized by immunofluorescence using anti-Myc antibody in XL2 cells (f and g; bottom panel). In mitotic cells Myc-TCTP accumulates in the spindle (f; here in metpahase. In interphase cells (g) Myc-TCTP forms a fibrous, MT-like network. Non transfected cells were entirely negative for anti-Myc antibody as shown in fig. 2C (negative cells around the central positive one). Bars = 20 μm. (B) Endogenous TCTP was visualized by immunofluorescence (a) in parallel with MTs (b) using monoclonal α-tubulin. The merged image (c) shows differences between TCTP and MTs fibers localization in the most flattened cell parts. Red arrows point out MTs which do not correspond to TCTP fibers and appear red. Bars in a–c = 20 μm. Higher magnifications of cells illustrate distinct TCTP (green) and MT (red) fibers (d–f). Green arrows show examples of TCTP fibers not overlapping with MTs and red arrows point out MTs free of TCTP. In colchicine-treated cells (e,f) MTs become less dense and the lack of colocalization between MTs and TCTP fibers is visible even in the cell body and not only in their most flattened parts. Note that most green TCTP fibers have no equivalent in MTs (green arrows in e and f). Inversely, most, if not all, MTs are free of TCTP (red arrows in e and f). Bars: in d = 10 μm, in e = 20 μm, in f = 15 μm. All cells in A and B were fixed with methanol/formaldehyde.

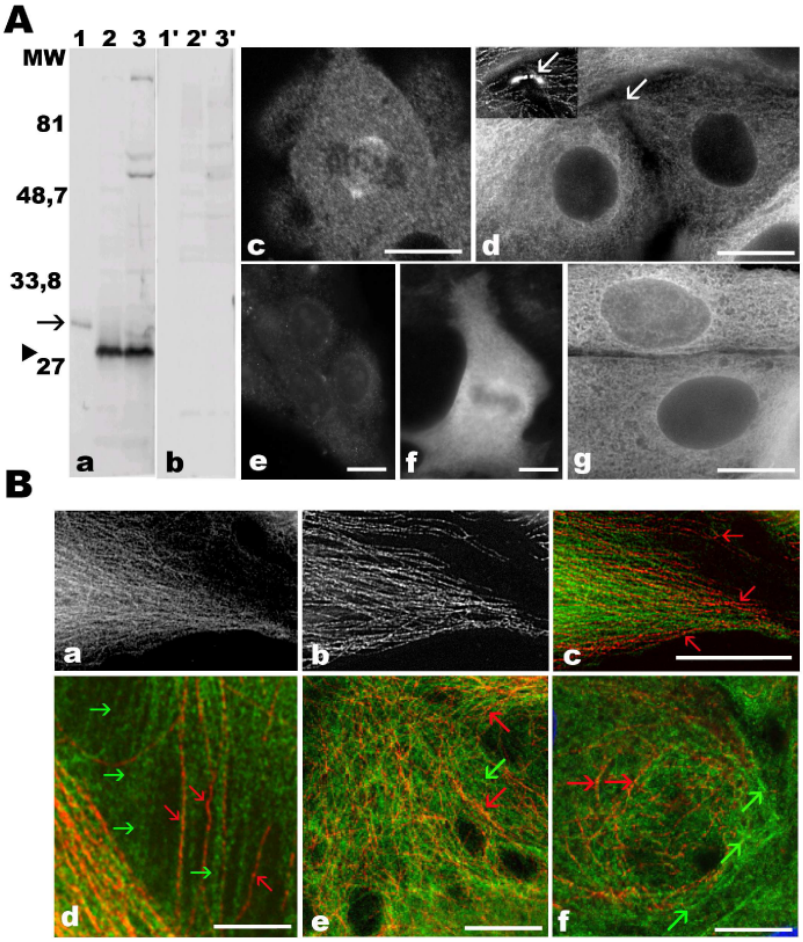

Fig. 2

TCTP is abundant in the mitotic spindle, but it is not associated with spindle microtubules

(A) Mitotic spindles were assembled in the CSF extract following addition of sperm heads and rhodamine-tubulin. Samples were frozen in liquid nitrogen, post-fixed in cold methanol (crude spindles) and stained for DNA (a), TCTP (b) and MTs (c; merged image in d). Spindles show high, but not fibrous TCTP staining and a granular network of TCTP in the adjacent cytoplasm which does not colocalize to microtubules (especially visible in corners of b, c and d). Two examples of MT fibers (black arrows in c) which do not correspond to any TCTP fibers (white arrows in b) are shown. In parallel, spindles assembled in the extract were purified on glycerol cushion, fixed (purified spindles), processed for DNA staining (e), TCTP immunofluorescence (f) and MTs labeling with rhodamine-tubulin (g; merged image in h). The majority of TCTP staining disappeared from purified spindles and discrete fluorescent dots of TCTP remained on the spindle poles (white arrows in f). Merged image of DNA, TCTP and rhodamine-tubulin (h) shows clear red staining of spindle MTs with yellow dots on its poles indicating that only in these areas the colocalization of TCTP and tubulin is detected. Inset in h shows details of a merged image of another spindle pole with TCTP remnants in higher magnification. Bars = 20 μm. (B) Either 6His-Xl TCTP or 6His-Xl TCTP$^{\Delta MAP1B}$ does not modify assembly/disassembly of MTs in vitro. Tubulin alone (control) or mixed with two concentrations of recombinant wild type TCTP (TCTP 2μM and 8 μM) or ΔMAP1B deletion mutant (ΔMAP1B 2μM and 8 μM) were incubated at 37°C (0–35 min.) or 4°C (35–60 min.) and optical density of samples was measured at 350-nm light wave to follow assembly (0–35 min.) and disassembly (35–60 min.) of MTs. All curves are very similar indicating that neither 6His-Xl TCTP nor 6His-Xl TCTP$^{\Delta MAP1B}$ modifies MTs dynamics. (C) MAP1 domain does not influence localization of TCTP. Myc-TCTP$^{\Delta MAP1B}$ localizes to mitotic spindles (b; here in metaphase) after expression in XL2 cells and forms a network in the cytoplasm of both mitotic (b) and interphasic cells (a). XL2 cells were transfected with an appropriate vector, cells were fixed and processed for anti-Myc immunofluorescence. Single confocal sections of DNA (blue) and anti-Myc immunofluorescence (red) in an interphase (a) and metaphase (b) cells are shown. Note that peripheral cells which do not express Myc-TCTP are negative while stained with anti-Myc antibody providing the control of the specificity of anti-Myc detection for the exogenous protein. Bars = 20 μm.

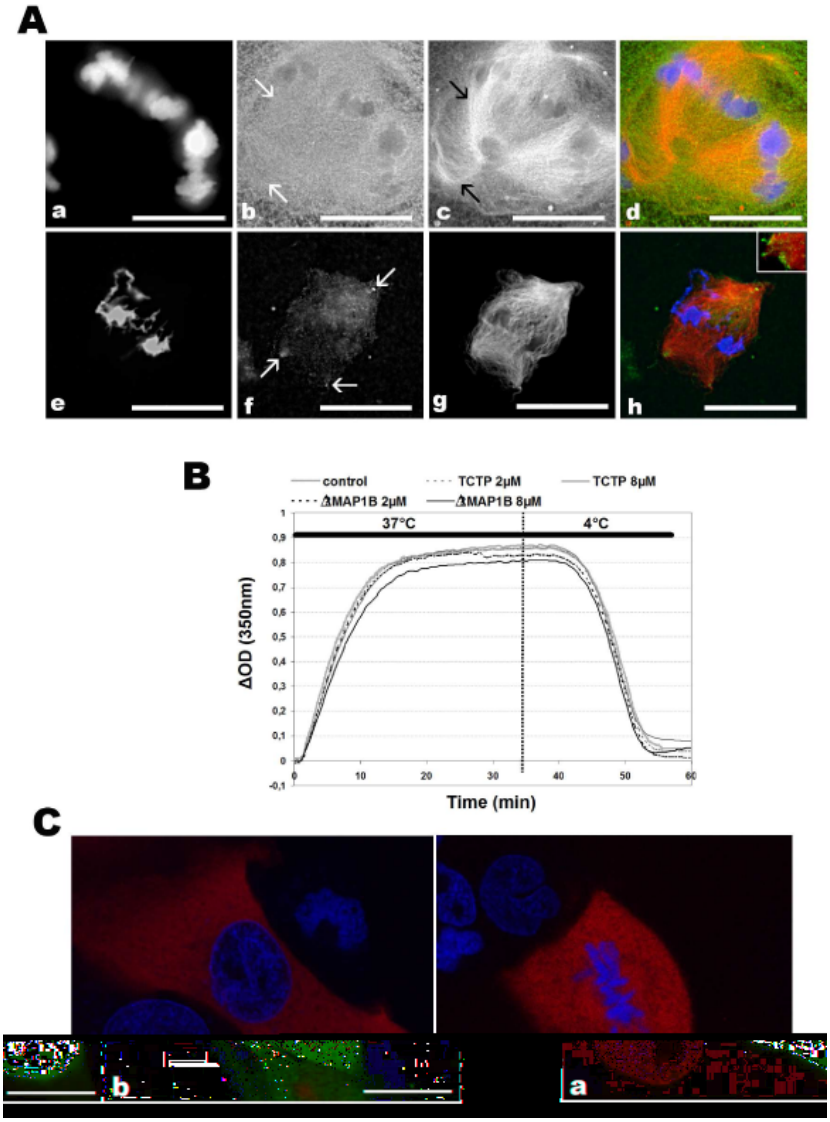

Fig. 3

Xl TCTP does not associate with taxol-stabilized MTs in co-sedimentation assay

(A) Recombinant 6His-Xl TCTP precipitates alone in MT-stabilizing buffer in concentration-dependent manner (0,5 and 2,5 mM). Proportions of TCTP in supernatants and pellets are similar in the two concentrations studied. (B) Taxol-stabilized microtubules alone precipitate in pellet (P) and lower supernatant (LS), while only traces of tubulin are detected by Western blotting in the upper supernatant (US; top row, right). The amount of TCTP is very similar in MT-devoid (−; left) and MT-containing pellet (+; right) (middle row) despite high accumulation of MTs in the pellet (P) and lower supernatant (LS). Proportions of control H2 fragment of CLIP-170 recombinant protein (known to bind to MTs; bottom row) in the supernatant and pellet change in relation with the presence of MTs. H2 is mostly accumulated in the lower supernatant (LS) while the lowest proportion was found in the pellet (P) in the absence of MTs (−). It is enriched in the pellet and diminishes in the upper (US) and lower (LS) supernatants in the presence of MTs (+) accordingly with the abundance of tubulin signal in each fraction (the very bottom of the Western blot). (C) Xl TCTP and Myc-Xl TCTP expressed in reticulocyte lysate are not enriched in the MTs-containing pellet. Xl TCTP (upper panel) and Myc-Xl TCTP (lower panel) were expressed in vitro in the lysate of rabbit reticulocytes. Taxol-stabilized MTs were added (+) or not (−) to the lysates expressing either of the two forms of Xl TCTP. Tubulin Western blots show that MTs accumulate specifically in the pellets (P; right in upper rows of both panels). TCTP Western blots show a very similar pattern of distribution of Xl TCTP and Myc-Xl TCTP respectively in the supernatants (S) and in the pellets (P) in the presence and absence of MTs (bottom rows in each panel respectively). The plasmid containing untagged Xl TCTP allows expression of TCTP (arrow) as well as an additional, non-identified protein visualized as a slower-migrating band present exclusively in the supernatants (S) also regardless of the presence of absence of MTs. Myc-Xl TCTP migrates as a single major band (arrow in the bottom row of the lower panel) which is predominantly found in the supernatants (S) and only as traces in the two type of pellets (P) regardless of presence or absence of MTs. Note that proportion of Myc-TCTP in the pellet (with or without MTs) is much less important than in the case of untagged TCTP. This suggests that Myc tag may limit oligomerization of TCTP. (D) Endogenous Xl TCTP from CSF and interphase extracts is not enriched in MTs pellet indicating that it does not associate with MTs. CSF and interphase extract were supplemented (+) or not (−) with taxol-stabilized MTs, incubated at 37°C, centrifuged and collected as upper supernatant (US), lower supernatant (LS) and pellet (P). No difference between CSF and interphase extract was observed. In the presence of taxol-stabilized MTs the pellet is enriched in MTs as indicated by the high signal on anti-tubulin Western blot (upper row, rightmost). Tubulin signal in LS and P in the absence of taxol-stabilized MTs comes from endogenous MTs and tubulin (−; left). The pattern of distribution of endogenous TCTP in US, LS and P fractions is rigorously the same in the absence (−; left) and presence (+; right) of taxol-stabilized MTs (middle row). Control endogenous protein, kinesin Eg5 (known to associate with MTs) is enriched in the pellet (P) in the presence of taxol-stabilized MTs (rightmost; bottom row) in parallel with enrichment in MTs. (E) Modulation of the quantity of MTs in pellets of CSF and interphase extracts does not modify the amount of endogenous pelleted Xl TCTP. Endogenous TCTP is found in rigorously the same proportions (left) between upper supernatant (US), lower supernatant (LS) and pellet (P) in control interphase and CSF extracts (+DMSO; upper row) in the presence either of taxol (middle row) or nocodazole (bottom row). Proportions of endogenous tubulin signal on Western blots corresponding to the same fractions (right) vary considerably. It is shifted in favour of the pellet in the presence of taxol (middle row) and has a tendency to diminish in the presence of nocodazole (bottom row).

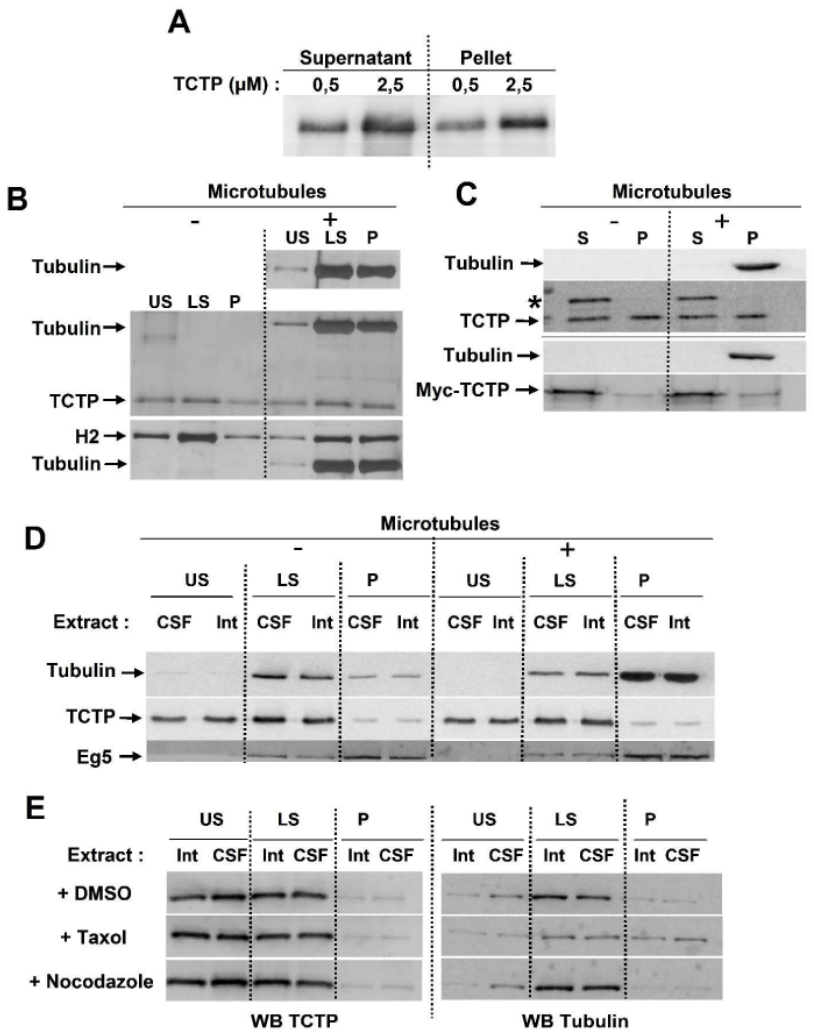
A
Supernatant
Pellet
TCTP (µM) :
0,5
2,5
0,5
2,5
B
Microtubules
-
+
US
LS
P
Tubulin
TCTP
H2
C
Microtubules
S
P
Myc-TCTP
D
Extract :
CSF
Int
Eg5
E
+ DMSO
+ Taxol
+ Nocodazole
WB TCTP
WB Tubulin

Fig. 4

TCTP colocalizes with F-actin in XL2 cells and has an affinity for F-actin fibers in a co-sedimentation assay with cell-free extracts

(A) TCTP forms curly fibers at the cell border in flattened and migrating XL2 cells (fixed with paraformaldehyde). Endogenous (left) and Myc-TCTP (right) shows distinct curly fibers at the cell border (arrows). (B) TCTP partially colocalizes with F-actin. Double staining for TCTP (left) and F-actin (right) in control (upper row) and cytochalasin D-treated (bottom row) cells fixed with paraformaldehyde. Note clear colocalization of TCTP and F-actin on the cells border in control cells. Cytochalasin D induces actin-rich foci (bottom, right) in which TCTP accumulates preferentially (bottom, left). TCTP (left) was immunolocalized, while F-actin was stained with phalloidin-rhodamin (right). Peripheral fibers in control cells in which TCTP and actin colocalize disappear after cytochalasin treatment. Bars = 20 μm. (C) Recombinant 6His-Xl TCTP is not enriched in F-actin containing pellet in vitro. Increasing concentrations (0,5; 1; 2,5 μM) of recombinant TCTP alone (−) were incubated in the buffer without F-actin and centrifuged (top row). Supernatants contain growing amounts of TCTP while a similar amount of TCTP is found in the pellet. When F-actin is added (+) to the mixture it is found exclusively in the pellets (middle row) while TCTP remains in unchanged proportions in supernatants and pellets in the same samples (+; bottom row) as in the absence of F-actin (top row). (D) Endogenous Xl TCTP is enriched in the pellet containing F-actin incubated both with CSF and interphase extracts similarly as endogenous tropomyosin known to associate with F-actin. F-actin was not added (−; left) or added (+; right) to CSF and interphase extracts. Endogenous actin is detected in upper (US) and lower (LS) supernatants (both in − and +). Exogenous F-actin is detected in the pellet (P) in F-actin supplemented extracts (top row; rightmost). TCTP is almost absent in the pellet (P) in the absence of exogenous F-actin (second row, − P), but it appears in the pellet (P) in the presence of exogenous F-actin (second row, + P). Tubulin Western blot was used as a negative control (third row). Tubulin is detected largely in the lower supernatant (LS) both in the absence and presence of exogenous F-actin (third row). Tropomyosin, used here as a positive control (bottom row), accumulates in the pellet (P) only in the presence of exogenous F-actin (bottom row, + P, righmost). Note that non-specific bands recognized by anti-tropomyosin antibody on the Western blot are not present in the pellet confirming the specificity of the assay (compare +P with + and − LS and US lanes).

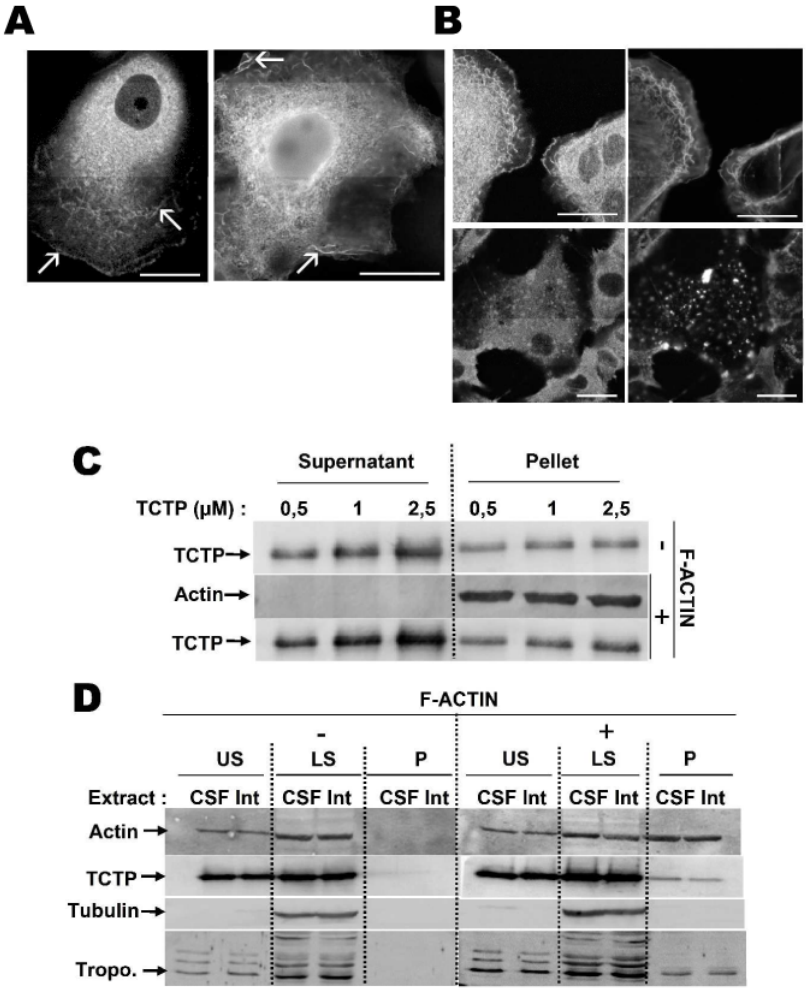

Fig. 5

Knockdown of Xl TCTP by siRNA induces drastic change in cell shape

(A) TCTP siRNA diminishes significantly the quantity of TCTP in XL2 cells (Western blot; left) and induces changes the their shape (Nomarski differential interference contrast; right). Western blot: untreated cells (−), HiPerfect-treated control cells (HiPerfect), siRNA-treated cells (RNAi TCTP). XL2 cells grow in islands of well attached cells (control). siRNA TCTP-treated cells are highly elongated and attached with each other only through very limited areas (RNAi TCTP). Bar = 40 μm. (B) Knockdown of Hs TCTP in HeLa cells by siRNA using either of three different oligonucleotides diminishes significantly the levels of TCTP protein (Western blot) and induces cells elongation and MT bundling (color images). Immunofluorescence: DNA, TCTP and MTs staining followed by merge of control cells (top row), the oligonucleotide A RNAi (second row) shows the mildest phenotype (TCTP signal diminishes in the cytoplasm and in mitotic spindles as well as some cells become elongated and form protrusions), oligonucleotide B (third row) gives the strongest phenotype (cells become long and fusiform, their proliferation slows down and longitudinal cables of MTs are formed in the cytoplasm), oligo C (bottom row) gives an intermediate phenotype (cells elongate, form protrusions and their proliferation is slowed down).

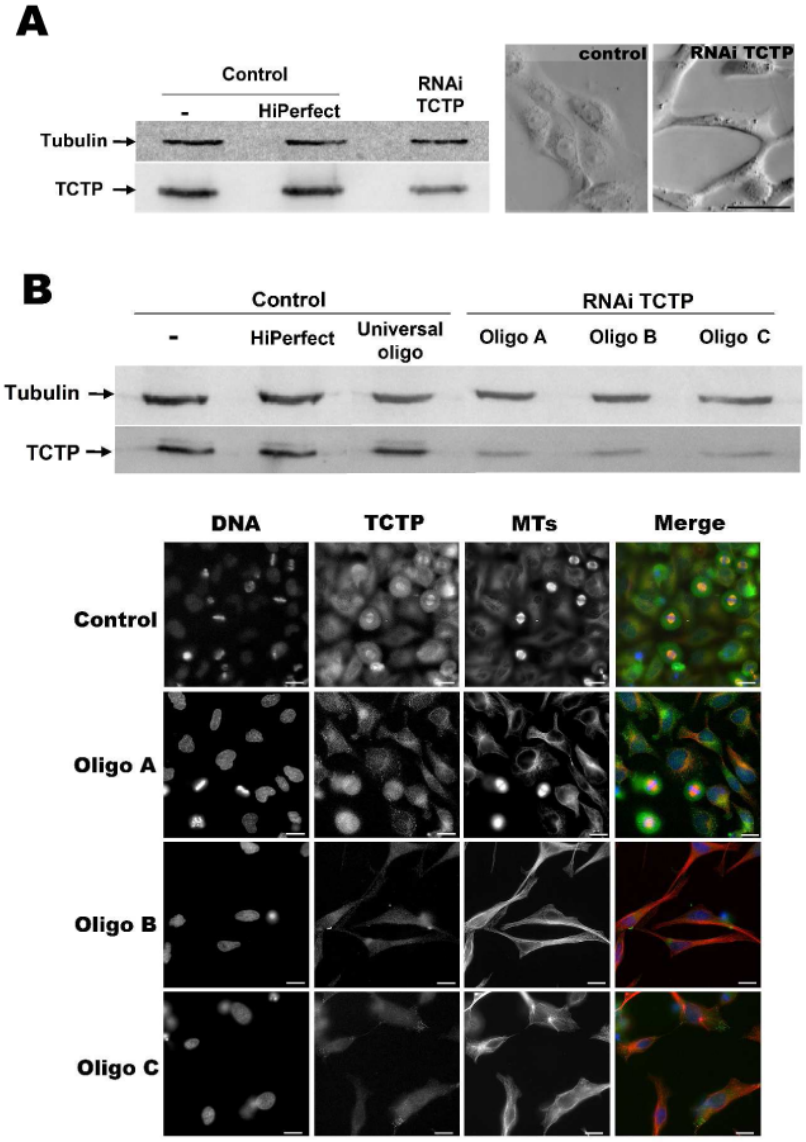

Fig. 6

Phenotype of HeLa cells upon TCTP knockdown

(A) Upon RNAi of TCTP the staining of TCTP disappears from the mitotic spindle and long protrusions formed during interphase may persist upon mitosis (DNA, TCTP, merge - from left to right). Top row - control. Second, third and bottom row - rounded mitotic cells treated with oligos A, B and C respectively in which spindle TCTP staining disappeared or diminished significantly (bottom). Fourth row - metaphase cell treated with oligo B with long protrusion oriented along the spindle axis. (B) Actin localization in control and TCTP siRNA-treated cells. Flattened cells with abundant cortical actin and stress fibers (control) transform into highly elongated ones (RNAi TCTP). Actin staining remains cortical with numerous fibers oriented perpendicularly to the cell axis. Bars = 20 μm. (C) Elongation of HeLa cells upon TCTP knockdown is MT-dependent. Control −: control cells. Control +: nocodazole-treated for 24 hours. Nocodazole increases the number of mitotic cells (rounded up) in comparison to the untreated control (−). Nocodazole treatment does not influence the shape of interphase cells which remain flattened (control +). In oligo B-treated cells (RNAi TCTP −) highly elongated interphase cells are present in the absence of nocodazole (−). The drug treatment (RNAi TCTP +) induces massive flattening of interphase cells, which become morphologically undistinguishable from the controls; compare interphase cells in control (−) with RNAi TCTP (+). Bar = 200 μm. (D) Cell protrusions induced by TCTP RNAi participate in unequal division of daughter cells during cytokinesis. The long protrusions (arrows) formed during interphase remain oriented along the spindle axis during mitosis. They participate in unequal mitotic division (compare the size of daughter cells upon cytokinesis of two dividing cells at 90 min time point. Arrows at 150 min time point show daughter cells which contain the protrusion. Photographs of time-lapse videomicroscopy of two dividing cells filmed during 150 min. Bars = 20μm.